machinery can physically interact with this tail (*9–11*). Proteins that bind to this tail have the potential to modulate CFTR gating by stabilizing or disrupting its interaction with the R domain. The NH_2-terminal tail of CFTR could serve as a target for physiologic regulators of CFTR gating or for pharmacologic maneuvers to modulate CFTR activity.

References and Notes

1. M. J. Welsh and A. E. Smith, *Cell* **73**, 1251 (1993).
2. S. E. Gabriel, K. N. Brigman, B. H. Koller, R. C. Boucher, M. J. Stutts, *Science* **266**, 107 (1994).
3. T. Baukrowitz, T. C. Hwang, A. C. Nairn, D. C. Gadsby, *Neuron* **12**, 473 (1994).
4. M. R. Carson, S. M. Travis, M. J. Welsh, *J. Biol. Chem.* **270**, 1711 (1995).
5. D. J. Wilkinson *et al.*, *J. Gen. Physiol.* **107**, 103 (1996).
6. S. H. Cheng *et al.*, *Cell* **66**, 1066 (1989).
7. C. E. Bear *et al.*, *ibid.* **68**, 809 (1992).
8. C. J. Matthews *et al.*, *J. Physiol. (London)* **508**, 365 (1998).
9. A. P. Naren *et al.*, *Nature* **390**, 302 (1997).
10. A. P. Naren *et al.*, *Proc. Natl. Acad. Sci. U.S.A.* **95**, 10972 (1998).
11. L. S. Prince *et al.*, *J. Biol. Chem.* **274**, 3602 (1999).
12. Cystic Fibrosis Genetic Analysis Consortium (www.genet.sickkids.on.ca/cftr).
13. All point mutations were introduced into a 1-kb fragment of the CFTR coding region by the Quickchange site-directed mutagenesis kit (Stratagene). This fragment was sequenced completely to verify each mutation and then ligated into pCDNA3 vector (Invitrogen) containing the rest of the CFTR coding region.
14. A. P. Naren, E. Cormet-Boyaka, K. L. Kirk, unpublished data.
15. A. P. Naren, M. Villain, D. Muccio, K. L. Kirk, unpublished data.
16. The triple and quadruple N-Tail mutants are not completely inactive; for example, cAMP-activated currents can be detected when higher cRNA amounts for these mutants are injected. Indeed, because of the nonlinearity of the oocyte expression system, the currents mediated by these mutants can approach (but not reach) wild-type levels at very high cRNA amounts (such as 50 ng).
17. J. Fu and K. L. Kirk, unpublished data.
18. S. H. Cheng *et al.*, *Cell* **63**, 827 (1990).
19. M. W. Quick and K. L. Kirk, unpublished data.
20. Recombinant NBD1 (amino acids 433 to 584) bound weakly to GST–N-Tail, but this binding was not inhibited by the N-Tail mutations that inhibit CFTR channel activity.
21. A. P. Naren and K. L. Kirk, unpublished data.
22. M. C. Winter and M. J. Welsh, *Nature* **387**, 294 (1997).
23. J. Ma, J. Zhao, M. L. Drumm, J. Xie, P. B. Davis, *J. Biol. Chem.* **272**, 28133 (1997).
24. Assays were done as described (*9, 10*). Briefly, soluble GST–N-Tail peptide was added to a lysate of COS-7 cells [0.2% Triton X-100 in phosphate-buffered saline (PBS)] transiently expressing recombinant CFTR (or various R domain constructs) and mixed for 1 hour at room temperature. Bound proteins were precipitated with excess glutathione agarose, washed extensively in 0.2% Triton X-100 in PBS, and analyzed for CFTR or R domain by immunoblotting with monoclonal antibodies to the COOH-terminus or R domain (Genzyme). CFTR immunoprecipitations were done on portions of the same lysates (*9, 10*).
25. Peptides were synthesized on a PerSeptive Biosystems 9050 peptide synthesizer. The biotin was conjugated to the NH_2-terminus with fluorenyl methoxycarbonyl-amino caproic acid as spacer. Peptide binding (biotin P30-63) was assessed by mixing 1.25 μM peptide and 2.5 μM soluble GST-R domain peptide in PBS for 1 hour at 22°C. A 100-fold molar excess of unbiotinylated peptide was used for competition experiments. The complex was precipitated with excess glutathione agarose and washed with PBS. Streptavidin–horseradish peroxidase (HRP, 1 μM) was added in PBS and incubated for 20 min. The beads were washed extensively in PBS plus 0.2% Triton X-100 and assayed for HRP activity with 2,2′-azinobis(3-ethylbenzothiozoline)-6 sulfonic acid (ABTS) according to manufacturer's instructions (Pierce, St. Louis, MO).
26. The single-channel properties of wild-type CFTR and the N-Tail mutants were analyzed in inside-out membrane patches excised from oocytes. The pipette solution contained 140 mM *N*-methyl-D-glucamine (NMDG), 0.2 mM $CaCl_2$, 0.5 mM $MgCl_2$, and 10 mM Hepes (pH to 7.4 with HCl). The bath solution contained 140 mM NMDG, 0.5 mM $MgCl_2$, 1 mM EGTA, and 10 mM Hepes (pH to 7.4 with HCl) supplemented with 1.5 mM Mg-ATP and PKA catalytic subunit (80 U/ml, Promega). Records of multichannel patches (holding potential −80 mV) were digitized using an Axopatch 200B amplifier, filtered at 200 Hz, and analyzed using PCLAMP 6.0 software. The open probabilities of the N-Tail mutants should be considered to be maximal estimates given the very brief open times of these mutants, which leads to underestimating channel number. Open-channel burst durations were estimated with the cycle time method and a minimal interburst duration of 20 ms (*8*). The N-Tail mutants also exhibited reduced open-channel burst durations relative to wild-type CFTR when analyzed at shorter minimal interburst durations such as 10 ms; however, this gave an underestimate of the true open-channel burst duration. The single-channel properties of the ΔR CFTR constructs were analyzed in membrane patches excised from transfected HeLa cells as described (*22*) with a minimal interburst duration of 20 ms. All patch clamp experiments were performed at 20° to 22°C.

27. We thank M. Welsh for providing the original ΔR-S660A CFTR construct. Supported by NIH grants DK51868 and DK50830 (K.L.K.), DA10509 (M.W.Q.), and MH52527 (J.E.B.).

1 June 1999; accepted 26 August 1999

Neurogenesis in the Neocortex of Adult Primates

Elizabeth Gould,* Alison J. Reeves, Michael S. A. Graziano, Charles G. Gross

In primates, prefrontal, inferior temporal, and posterior parietal cortex are important for cognitive function. It is shown that in adult macaques, new neurons are added to these three neocortical association areas, but not to a primary sensory area (striate cortex). The new neurons appeared to originate in the subventricular zone and to migrate through the white matter to the neocortex, where they extended axons. These new neurons, which are continually added in adulthood, may play a role in the functions of association neocortex.

The traditional view of the adult primate neocortex is that it is structurally stable and that neurogenesis and synapse formation occur only during development (*1, 2*). Yet structural plasticity in adult brains is found both among lower vertebrates (*3*) and in phylogenetically older mammalian structures such as the olfactory bulb and hippocampus (*4, 5*), even in primates (*6, 7*). Furthermore, neurogenesis is widespread in the adult avian brain including in the hyperstriatum (*8, 9*), a structure homologous to the mammalian cerebral cortex (*10*). Thus, it may seem paradoxical that there is no compelling evidence for neurogenesis in the neocortex of adult mammals (*11*) and there are even strong claims against it for primates (*1*). Using bromodeoxyuridine (BrdU) labeling, which marks proliferating cells and their progeny (*12*), combined with retrograde tract tracing and immunohistochemistry for neuronal markers, we attempted to resolve this paradox. We report that in adult macaques, new neurons are indeed added to several regions of association cortex where they extend axons. The presence of new neurons in brain areas involved in learning and memory (*13*) supports earlier suggestions that adult-generated neurons may play a role in these functions (*9, 14, 15*).

We injected 12 adult *Macaca fascicularis* with BrdU and used immunohistochemistry for cell-specific markers to examine BrdU-labeled cells in prefrontal, inferior temporal, posterior parietal, and striate cortex (*16*). The following markers were used: for mature neurons, (i) NeuN (neuronal nuclei), (ii) NSE (neuron-specific enolase), or (iii) MAP-2 (microtubule-associated protein-2); for immature neurons, TOAD-64 (turned-on-after-division 64-kD protein); for astroglia, GFAP (glial fibrillary acidic protein) (*17, 18*).

In animals perfused 1 week or more after the last BrdU injection, we observed BrdU-labeled cells in prefrontal, inferior temporal, and parietal cortex (Figs. 1 and 2; Table 1). In the region of the principal suicus in prefrontal cortex, the majority (62% to 84%) of BrdU-labeled cells had round or oval nuclei, morphological characteristics of mature neurons (nuclear diameter = 10 to 25 μm). Confocal laser scanning microscopic analysis of immunostained tissue (*19*) indicated that a subset of these cells expressed markers of mature neurons (Figs. 1 through 3; Table 1). BrdU-

Department of Psychology, Princeton University, Princeton, NJ 08544, USA.

*To whom correspondence should be addressed. E-mail: goulde@princeton.edu

labeled cells with neuronal characteristics were found in layers 1 through 5, but not 6. Those that were immunoreactive for MAP-2 exhibited dendritic processes (Fig. 3).

Similar proportions of BrdU-labeled cells were co-labeled with the neuronal marker NeuN in inferior temporal cortex (animals #4 and #5), posterior parietal cortex (#10, #11, #12), and in the vicinity of the anterior cingulate sulcus (#5). In contrast, very few BrdU-labeled cells in these regions co-labeled with a marker of astroglia, GFAP (Fig. 3; Table 1). Unlike the association cortex areas examined, in striate cortex, the few BrdU-labeled cells found never co-labeled with the neuronal markers, although some were positive for GFAP (#3, #4, #10, #11, #12). The absence of new neurons in striate cortex was probably not the result of either their rapid death or a longer migration time to reach striate cortex, because they were absent in animals perfused from 1 to 7 weeks after the first BrdU injection.

In the animals (#1, #2) that were perfused 2 hours after a single BrdU injection, labeled cells were observed in the subventricular zone (svz) lining the wall of the lateral ventricles (Fig. 4). In these animals, very few BrdU-labeled cells were observed in the neocortical areas examined; all had small, irregularly shaped nuclei and none expressed neuronal markers. In animals that received several BrdU injections with survival times ranging from 1 to 3 weeks, we not only found BrdU-labeled cells in the svz but also observed evidence of migrating BrdU-labeled cells in the white matter of frontal and temporal sections (Figs. 4 and 5). The BrdU-labeled cells in the white matter were elongated or fusiform in shape, and those that were co-labeled with TOAD-64 had leading and trailing processes characteristic of migrating cells (Fig. 5) (*20*). In animals #3, #4, #5, and #7, these putative migrating cells were arrayed in a stream from their likely site of origin in the wall of the lateral ventricle, through the white matter, to their probable destination in frontal neocortex (Figs. 4 and 5). Elongated BrdU-labeled cells in the white matter did not co-label with markers of mature neurons or astroglia. This putative migratory route for newly generated cells was also observed in two additional animals that received a single BrdU injection and were perfused either 1 week (#8) or 2 weeks (#9) later (Table 1, Fig. 4).

These results suggest that in the adult macaque brain, new cells originate in the svz and migrate through the white matter to certain neocortical regions where they differentiate into mature neurons. At a short survival time (2 hours), BrdU-labeled cells were observed in the svz. At longer survival times (1 to 3 weeks), BrdU-labeled cells that appeared to be migrating were observed in the white matter, and

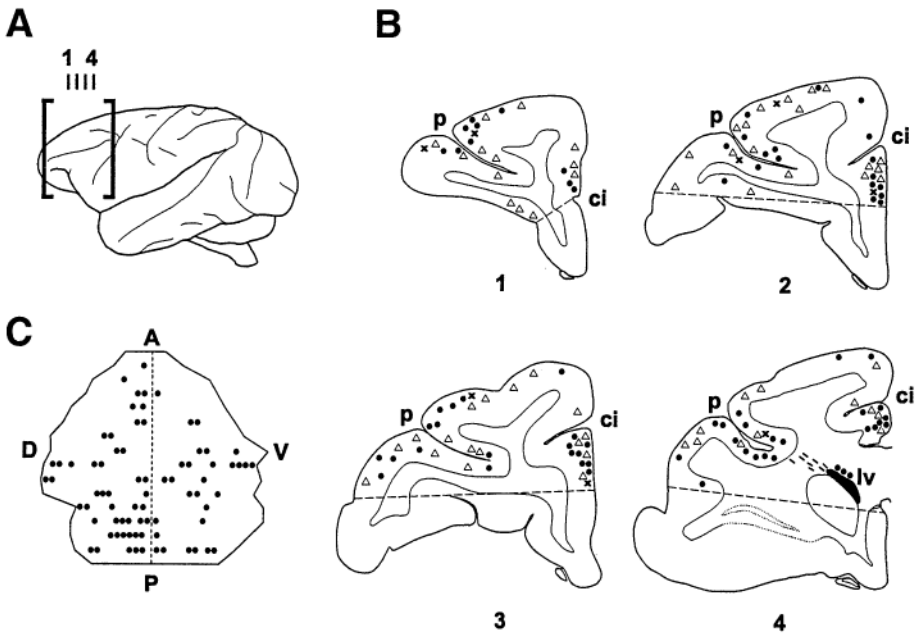

Fig. 1. The distribution of BrdU-labeled cells in prefrontal cortex in adult macaques. (**A**) Lateral view showing levels (1 through 4) of the coronal sections shown in (B) and the principal sulcus region (boxed area) from which the flattened map shown in (C) was made. (**B**) Coronal sections [adapted from (*30*)] showing the distribution of BrdU-labeled cells in the region of the principal sulcus and the anterior cingulate sulcus from animal #5. Solid dots represent BrdU-labeled cells that were not immunoreactive for NeuN or GFAP. Open triangles represent BrdU-labeled cells that were immunoreactive for the neuronal marker NeuN. X represents BrdU-labeled cells that were immunoreactive for the astroglial marker GFAP. Dashes (−) represent BrdU-labeled cells with elongated nuclei in the white matter. Regions below the dashed lines were not examined. ci, cingulate sulcus; lv, lateral ventricle; p, principal sulcus. (**C**) Flattened map of the principal sulcus region (#3) showing the distribution of BrdU-labeled cells (in coronal sections 1 mm apart). The dashed line represents the floor of the sulcus. Each dot represents one BrdU-labeled cell. There were no obvious dorsal-ventral or anterior-posterior gradients in BrdU-labeled cells in this area. A, anterior; V, ventral; D, dorsal; P, posterior.

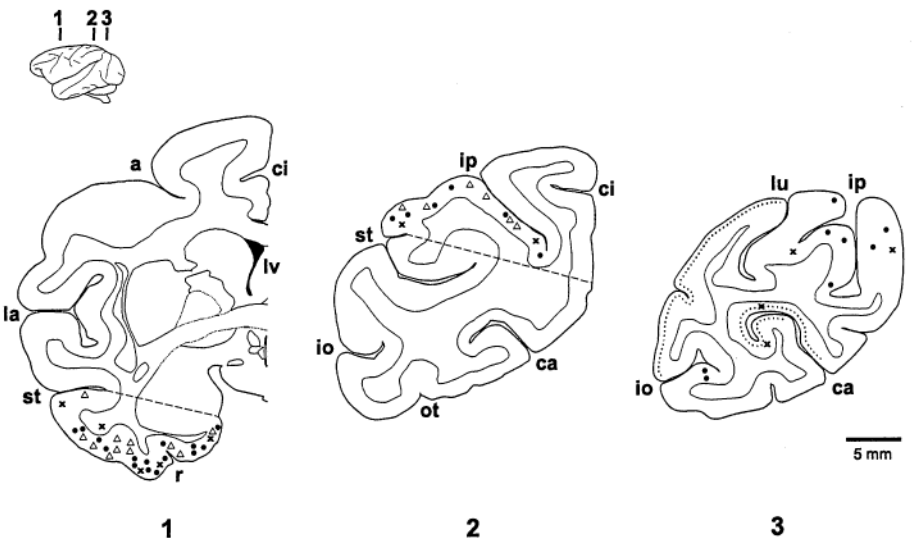

Fig. 2. The distribution of BrdU-labeled cells in coronal sections through inferior temporal cortex (section 1), posterior parietal cortex (section 2), and occipital cortex (section 3) (from animal #10). Symbols are as in Fig. 1. BrdU-labeled cells co-labeled with NeuN were not observed in striate cortex (shown with dotted lines in section 3). a, arcuate sulcus; ca, calcarine sulcus; io, inferior occipital sulcus; ip, intraparietal sulcus; la, lateral sulcus; lu, lunate sulcus; ot, occipito-temporal sulcus; r, rhinal sulcus; st, superior temporal sulcus. The area above the dashed line in 1 and below the dashed line in 2 was not analyzed.

those with mature neuronal characteristics were found in the neocortex. In the adult rodent, the svz produces new cells that migrate in the rostral migratory stream to the olfactory bulb, where they differentiate into neurons (*5*). Our results suggest that in the adult macaque, the svz is the source of an additional population of new neurons that migrate through fiber tracts to neocortical regions.

To establish further the neuronal identity of the new cells and explore their cortical connections, we carried out a combined BrdU labeling and fluorescent retrograde tracing study in animals #10, #11, and #12 (*21*). Several weeks after BrdU administration, these animals were

Table 1. Characteristics of experimental animals and BrdU-labeled cells in the principal sulcus region. All animals, except #7, were given one to five i.p. injections (injs.) daily of 75 to 100 mg/kg BrdU. For all animals but #7, survival time represents the time after the last BrdU injection when the monkey was perfused. Animal #7 received four i.v. injections of 100 mg/kg BrdU, each separated by 1 week with the last injection 24 hours before perfusion. Animals #1 to #6 were also used in a different study of neurogenesis in the dentate gyrus (*7*). The stereological optical dissector method was used to estimate the number of BrdU-labeled cells/mm^3 (*19*). The percentages of BrdU-labeled cells that expressed specific markers were each obtained from a sample of 100 BrdU-labeled cells per marker per animal. As mentioned in the text and in (*22*), three additional male animals (#10, #11, #12) were used for a retrograde tracer study and for identifying new neurons.

No. (sex)	Age (years)	BrdU injs.	Survival time	Percent BrdU-labeled cells				Number of BrdU-labeled cells/mm^3
				NeuN	NSE	MAP-2	GFAP	
1 (m)	5	1	2 hours	0	0	0	20	0.4
2 (m)	16	1	2 hours	0	0	0	31	0.6
3 (m)	5	5	2 weeks	52	43	37	5	26.5
4 (f)	7	5	2 weeks	47	39	33	8	13.2
5 (m)	10	3	1 week	38	32	26	4	17.6
6 (f)	15	5	2 weeks	–	28	–	2	13.7
7 (m)	15	4	24 hours	53	48	29	3	15.6
8 (m)	5	1	1 week	–	–	–	–	7.2
9 (m)	5	1	2 weeks	–	–	–	–	14.4

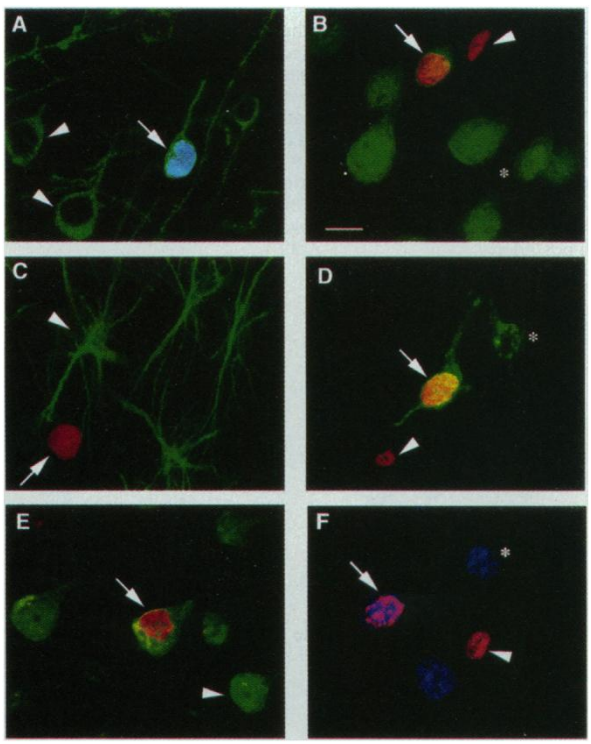

Fig. 3. Confocal laser scanning microscopic images of BrdU-labeled cells in the adult macaque neocortex. (**A**) Arrow: prefrontal cell with neuronal morphology co-labeled for BrdU (blue nuclear stain, cascade blue) and MAP-2 (green cytoplasmic stain, Alexa 488). Arrowheads: BrdU-negative, MAP-2 positive cells (animal #4). (**B**) Arrow: prefrontal cell with neuronal morphology co-labeled for NeuN (green nuclear and cytoplasmic stain, Alexa 488) and BrdU (red nuclear stain, Alexa 568). Arrowhead: cell positive for BrdU, not for NeuN. Asterisk: cells positive for NeuN, negative for BrdU (#3). (**C**) Arrow: prefrontal cell with neuronal nuclear morphology positive for BrdU (red nuclear stain), not stained for the astroglial marker GFAP. Arrowhead: cell with astrocyte morphology negative for BrdU, positive for GFAP (green stain) (#5). (**D**) Arrow: prefrontal cell in ventral principal sulcus with neuronal morphology co-labeled with BrdU (red nuclear stain) and Fluoro-Emerald (green cytoplasmic marker). The tracer was injected into the dorsal bank of principal sulcus (#11). This cell was outside of the injection site diffusion zone. Arrowhead: BrdU-positive cell (red nuclear stain) not labeled with Fluoro-Emerald. Asterisk: Fluoro-Emerald–labeled cell which is BrdU-negative. (**E**) Arrow: posterior parietal cell co-labeled for NeuN (green nuclear and cytoplasmic stain) and BrdU (red nuclear stain). This cell has the morphology of a pyramidal cell (#12). Arrowhead: NeuN-positive, BrdU-negative cell. (**F**) Arrow: posterior parietal cell co-labeled with BrdU (red nuclear stain) and the retrograde tracer Fast Blue (blue cell-body marker). The tracer was injected into area 7A. This cell was outside of the injection site diffusion zone (#12). Arrowhead: BrdU-labeled cell not labeled with Fast Blue. Asterisk: Fast Blue–labeled cell not co-labeled with BrdU. Scale in (B) = 20 μm and applies to all frames.

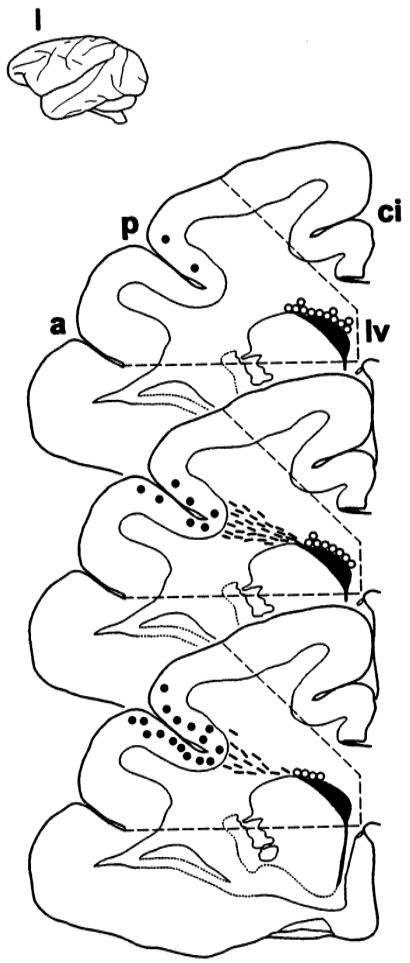

Fig. 4. The distribution of BrdU-labeled cells in animals that were perfused 2 hours (top section, animal #1), 1 week (middle section, #8), and 2 weeks (bottom section, #9) after a single BrdU injection, showing the putative migration of new cells from the svz to the principal sulcus. Area within the dashed lines represents analyzed region. Open circles represent BrdU-labeled cells in the svz. Dashes (–) represent BrdU-labeled cells in the white matter, the majority of which had fusiform nuclei. Solid dots represent BrdU-labeled cells in the cortex surrounding the principal sulcus. Vertical line above lateral view of the brain marks the approximate level of the section shown for each of the three animals.

injected with Fluoro-Emerald in lateral prefrontal cortex (Area 46) and with Fast Blue in posterior parietal cortex (Area 7A) (*22*). These injection sites were chosen because both are known projection targets of neurons in areas in which we had found BrdU-labeled cells, including lateral prefrontal, posterior parietal, and inferior temporal cortex (*23*). We observed cells labeled with BrdU that were retrogradely filled with either Fluoro-Emerald (in frontal cortex) or Fast Blue (in parietal cortex), providing further evidence that some new cells were neurons. Although tracer was transported from the injection sites to non–BrdU-labeled cells in frontal, parietal, and inferior temporal cortex, cells co-labeled with BrdU and tracer were only found within 11 mm of the border of the diffusion zone surrounding the injection sites. Thus, adult-generated cells in prefrontal and posterior parietal cortex extend short axons and may be incorporated into the local circuitry, although the existence of longer connections cannot be ruled out.

Although most neocortical neurons are generated prenatally (*24*), our findings indicate that neurons are added to primate neocortex in adulthood. We observed a considerable number of BrdU-labeled cells with neuronal characteristics, but the numbers generated daily in adulthood are presumably much higher because BrdU is only available for uptake for 2 hours after each injection (*12*). Thus, a single BrdU injection labels a fraction of the cells that divide in 24 hours. Furthermore, it is unlikely that the cells we observed incorporated BrdU during apoptosis, a phenomenon observed in both the developing neocortex and non-neuronal systems (*25*), because many labeled cells were present in neocortex weeks after the last BrdU injection without any signs of degeneration.

Our results are at variance with previous [^{3}H]thymidine autoradiographic studies which claim no neurogenesis in the adult primate neocortex (*1*). This discrepancy may be due to methodological differences. First, since ^{3}H penetrates only 1 to 3 μm into a tissue section, [^{3}H]thymidine autoradiography may underestimate the number of new cells (*26*). Furthermore, the previous study used much longer survival times (3 months to 6 years) for 9 of the 12 animals. New cells that incorporated [^{3}H]thymidine and differentiated into neurons may have died in the interval between injection and perfusion. This is supported by findings that many adult-generated hippocampal neurons die in animals not exposed to complex experiences (*17, 27*). Finally, all of the adult animals in the previous study were pregnant at the time of BrdU injection; pregnancy increases the level of circulating glucocorticoids (*28*), which in turn may inhibit cell proliferation (*29*).

Prefrontal, posterior, parietal, and inferior temporal cortex are areas involved in behavioral plasticity (*13*). Thus, it is conceivable that the new neurons added to these areas in adulthood might play a special role in such functions. Perhaps immature neurons are capable of undergoing structural changes rapidly and therefore may serve as a substrate for learning (*15*). Furthermore, the addition of new neocortical neurons throughout adulthood provides a continuum of neurons of different ages that may form a basis for marking the temporal dimension of memory. The idea that late-generated neurons play an important role in learning and memory was proposed previously by Altman (*14*), and, for the avian forebrain, by Nottebohm (*9*), but direct evidence is still lacking (*15*).

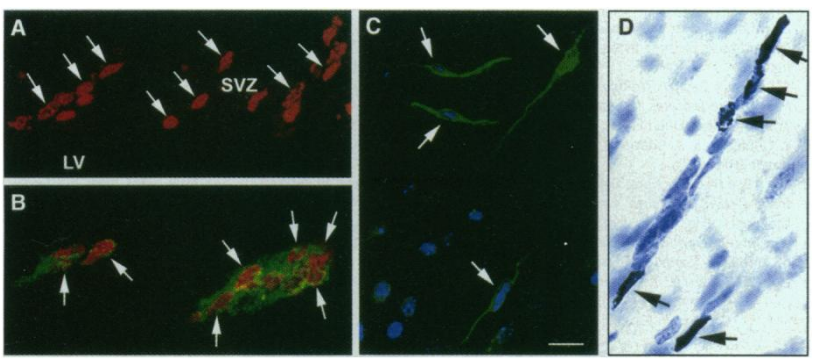

Fig. 5. Immature and migrating cells in the svz and subcortical white matter of adult macaques. (**A**) Arrows: confocal laser scanning microscopic image of chains of BrdU-labeled cells (red nuclear stain Alexa 568) in the svz (#11). (**B**) Arrows: confocal image of BrdU-labeled cells (red nuclear stain) that are TOAD-64–positive (green cytoplasmic stain, Alexa 488). These cells are organized in a chain on the border of the svz and the white matter (#10). (**C**) Arrows: confocal image of TOAD-64–positive cells (green cytoplasmic stain) with the morphology of immature neurons that appear to be migrating from the svz through the white matter to prefrontal cortex (#4). The blue nuclear stain is the DNA dye Hoechst 44323. (**D**) Light photomicrograph of BrdU-labeled cells (arrows) that appear to be migrating in a stream through the subcortical white matter (#4). Scale in (C) = 30 μm and applies to all frames.

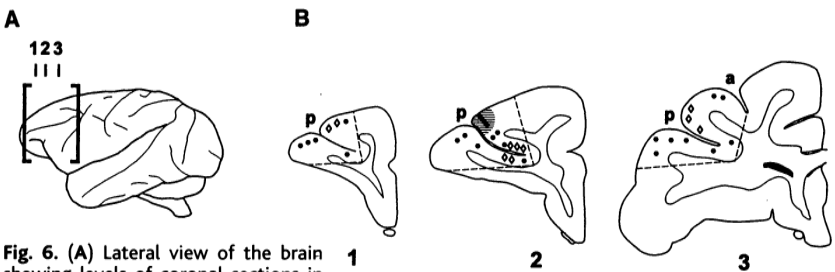

Fig. 6. (**A**) Lateral view of the brain showing levels of coronal sections in (B). (**B**) The distribution of BrdU-labeled cells in the principal sulcus from an animal (#10) that received an injection of the retrograde tracer Fluoro-Emerald into dorsal principal sulcus. The area within the dashed lines represents the analyzed region. Solid dots represent BrdU-labeled cells that were not co-labeled with retrograde tracer. Open diamonds represent BrdU-labeled cells that were retrograde-labeled with Fluoro-Emerald. Section 2 shows the middle of the injection site (solid line) surrounded by the diffusion zone (shaded area).

References and Notes

1. P. Rakic, *Science* **227**, 1054 (1985); *Ann. N.Y. Acad. Sci.* **457**, 193 (1985); *Nature Neurosci.* **1**, 645 (1998).
2. J. P. Bourgeois, P. S. Goldman-Rakic, P. Rakic, *Cereb. Cortex* **4**, 78 (1994).
3. For example, C. Lopez-Garcia *et al.*, *Brain Res.* **471**, 167 (1988); A. Alvarez-Buylla and C. Lois, *Stem Cells* **13**, 263 (1995).
4. For example, J. Altman and G. D. Das, *J. Comp. Neurol.* **124**, 319 (1965); M. S. Kaplan and J. W. Hinds, *Science* **197**, 1092 (1977); E. Gould *et al.*, *J. Neurosci.* **17**, 2492 (1997).
5. For example, J. Altman, *J. Comp. Neurol.* **137**, 433 (1969); L. Rosselli-Austin and J. Altman, *J. Dev. Physiol.* **1**, 295 (1979); P. Rousselot, C. Lois, A. Alvarez-Buylla, *J. Comp. Neurol.* **351**, 51 (1995); F. Doetsch, J. M. Garcia-Verdugo, A. Alvarez-Buylla, *J. Neurosci.* **17**, 5046 (1997).
6. E. Gould, P. Tanapat, B. S. McEwen, G. Flugge, E. Fuchs, *Proc. Natl. Acad. Sci. U.S.A.* **95**, 3168 (1998); P. S. Eriksson *et al.*, *Nature Med.* **4**, 1313 (1998).
7. E. Gould *et al.*, *Proc. Natl. Acad. Sci. U.S.A.* **96**, 5263 (1999).
8. For example, A. Alvarez-Buylla, C.-Y. Ling, F. Nottebohm, *J. Neurobiol.* **23**, 396 (1992); S. A. Goldman and F. Nottebohm, *Proc. Natl. Acad. Sci. U.S.A.* **80**, 2390 (1983); J. A. Paton and F. N. Nottebohm, *Science* **225**, 1046 (1984); A. Alvarez-Buylla and F. Nottebohm, *Nature* **335**, 353 (1988).
9. For example, A. Barnea and F. Nottebohm, *Proc. Natl. Acad. Sci. U.S.A.* **93**, 714 (1996); F. Nottebohm, *Ann. N.Y. Acad. Sci.* **457**, 143 (1985); ———, in *Neural Control of Reproduction*, J. M. Lakoski *et al.*, Eds. (Liss, New York, 1989), pp. 583–601.
10. W. J. H. Nauta and H. J. Karten, in *The Neurosciences: Second Study Program*, F. O. Schmitt, Ed. (Rockefeller Univ. Press, New York, 1970), pp. 7–25.
11. There are earlier reports of addition of cells to neocortex of adult rats and cats [for example, J. Altman, *Anat. Rec.* **145**, 573 (1963); M. S. Kaplan, *J. Comp.*

Neurol. **195**, 323 (1981)]. These studies, however, did not convincingly identify the new cells as neurons. Other claims of increased numbers of neocortical neurons after birth involve immature animals, brain-damaged animals, or both [for example, N. Sugita, *ibid.* **29**, 61 (1918); B. Kolb *et al.*, *Behav. Brain Res.* **91**, 127 (1998); W. R. Shankle *et al.*, *J. Theor. Biol.* **191**, 115 (1998); D. W. Pincus *et al.*, *Clin. Neurosurg.* **44**, 17 (1997)].

12. R. S. Nowakowski, S. B. Lewin, M. W. Miller, *J. Neurocytol.* **18**, 311 (1989).
13. For example, P. S. Goldman-Rakic, in *Handbook of Physiology, The Nervous System*, F. Plum, Ed. (American Physiological Society, Bethesda, MD, 1987), sec. 1, vol. 5, pp. 373–417; E. K. Miller, C. A. Erikson, R. Desimone, *J. Neurosci.* **16**, 5154 (1996); C. G. Gross, *Handbook of Sensory Physiology*, R. Jung, Ed. (Springer-Verlag, Berlin, 1993), vol. VII/3B, pp. 451–482; R. Andersen, in *Handbook of Physiology, The Nervous System*, F. Plum, Ed. (American Physiological Society, Bethesda, MD, 1987), sec. 1, vol. 5, pp. 483–518.
14. J. Altman, in *The Neurosciences: A Study Program*, G. C. Quarton, T. Melnechuk, F. O. Schmitt, Eds. (Rockefeller Univ. Press, New York, 1967), pp. 723–743.
15. E. Gould, P. Tanapat, N. B. Hastings, T. J. Shors, *Trends Cogn. Sci.* **3**, 186 (1999).
16. Macaques #1 to #9 were injected i.p. or i.v. with BrdU (75 to 100 mg/kg body weight), one to five times, and 2 hours to 3 weeks later were perfused under Nembutal anesthesia with 4.0% paraformaldehyde in 0.1 M phosphate buffer (Table 1). The 2-hour survival time was selected because it is sufficient for uptake of BrdU into cells in S-phase but not for mitosis or migration to occur (*12*). The 1- to 3-week survival times were used to maximize the chance of observing new cells that express neuronal markers and minimize the likelihood that new cells would die in the interval between labeling and perfusion. Macaques #10 to #12 were used in a combined BrdU labeling and retrograde tracing study. They were injected i.p. with 75 mg/kg BrdU at weekly intervals. Animal #10 (6 years old) was injected with BrdU four times and received the tracer 3 weeks after the first BrdU injection, animal #11 (6 years old) was injected six times and received the tracer injection 5 weeks after the first BrdU injection, and animal #12 (5 years old) was injected four times and received the tracer 6 weeks after the first BrdU injection. At 1 week after the tracer injections, these animals were perfused as described above. The tracer injections are described in the text and in (*22*).
17. G. Kempermann, H. G. Kuhn, F. H. Gage, *Nature* **386**, 493 (1997).
18. H. A. Cameron *et al.*, *Neuroscience* **56**, 337 (1993); L. S. Honig, K. Herrman, C. J. Shatz, *Cereb. Cortex* **6**, 794 (1996); J. E. Minturn *et al.*, *J. Comp. Neurol.* **355**, 369 (1995). Sections (40 μm) were cut coronally or horizontally through the prefrontal cortex for stereological analysis. Similar coronal sections were cut through portions of inferior temporal, posterior parietal, and striate cortex. To obtain stereological estimates of the total numbers of BrdU-labeled cells, tissue was processed immunohistochemically for BrdU alone using peroxidase methods. To determine the phenotype of BrdU-labeled cells, tissue was processed immunohistochemically for BrdU and one of several cell-specific markers, using fluorescent techniques. Sections from all brain regions were processed simultaneously to minimize variability. For BrdU peroxidase staining, tissue was heated in citric acid buffer, incubated in hydrogen peroxide, trypsin, and 2 M HCl, blocked in normal serum, and incubated in mouse anti-BrdU (1:100; Novocastra). Sections were processed using a Vectastain Elite ABC kit. These sections were then counterstained with cresyl violet and coverslipped under Permount. For immunofluorescence, tissue was pretreated for BrdU staining followed by incubation in mouse or rat anti-BrdU (1:200, Accurate Chemical). Subsequently, the sections were incubated in either biotinylated anti-mouse or anti-rat followed by Avidin-Neutralite-Cascade Blue (1:500, Molecular Probes) or Streptavidin-Alexa 568 (1:1000, Molecular Probes). These sections were then incubated in one of the following primary antisera: mouse anti-NeuN (1:100; Chemicon), rabbit anti-NSE (1:5000, Polysciences), mouse anti-MAP-2 (1:100, Chemicon), rabbit anti-TOAD-64 (1:10,000, gift of S. Hockfield, Yale University), or goat anti-GFAP (1:1000; Santa Cruz Biotech) and reacted with either goat anti-mouse Alexa 488 (1:500, highly cross-adsorbed, Molecular Probes), goat anti-rabbit Alexa 488 (1:500, Molecular Probes), or donkey anti-goat Alexa 488 (1:500, Molecular Probes), rinsed, dried, and coverslipped with glycerol:phosphate-buffered saline (3:1 v/v in 0.1% *N*-propyl gallate). Some sections were counterstained with the DNA dye Hoechst 44323 (Sigma) or treated with ribonuclease and stained with the DNA/RNA dye To-pro 3 (Molecular Probes). Control sections were processed as described above with omission of the primary antisera.
19. A modified version of the stereological optical dissector method [M. J. West, L. Slomianka, H. J. Gundersen, *Anat. Rec.* **231**, 482 (1991)] was performed on peroxidase-stained tissue on coded slides. For every 20th section through the principal sulcus, the number of labeled cells in both banks of the sulcus was determined using an Olympus BX-60 OptiPlex computer. Labeled cells were counted excluding those in the outermost focal plane to avoid counting cell caps. The total volume of the principal sulcus area was estimated with Stereoinvestigator (MicroBrightField). The data were expressed as number of BrdU-labeled cells/mm^3. Immunofluorescent tissue was viewed with an Olympus BX-60 fluorescent microscope and with a confocal laser scanning microscope (Zeiss 510 LSM) for verification of double labeling. Z-sectioning was performed at 1-μm intervals, and optical stacks of three to six images were produced for figures.
20. S. Ramon y Cajal, *Histology of the Nervous System of Man and Vertebrates*, N. Swanson and L. W. Swanson, Trans. (Oxford Univ. Press, Oxford, 1995), vol. 2.
21. E. Gould, M. S. A. Graziano, A. J. Reeves, C. G. Gross, unpublished data.
22. For the tracer injections, 0.4 μl of 2% Fluoro-Emerald tracer (Molecular Probes) was injected into the edge of the dorsal (Fig. 6) or ventral bank of the posterior portion of the principal sulcus (Area 46) or 0.4 μl of 2% of Fast Blue (Sigma) into the approximate center of exposed Area 7A. The injections were made with a Hamilton syringe over a 20-min period at a depth of 1 mm using a Zeiss binocular microscope. For both injections, the cortex was exposed under strictly aseptic conditions and deep isofluorothane anesthesia. After the injections, the surgical opening was closed and, 1 week later, the animal was perfused under deep Nembutal anesthesia (*16*). The tissue was processed for BrdU immunofluorescence (*18*) with Streptavidin-Alexa 568 (1:2,000, Molecular Probes). Only cells outside of the diffusion zone surrounding the injection site (in which both glia and neurons were labeled with the tracer) were examined for BrdU and retrograde tracer labeling.
23. D. S. Melchitzky *et al.*, *J. Comp. Neurol.* **390**, 211 (1998); R. A. Andersen, C. Asanuma, W. M. Cowan, *ibid.* **232**, 443 (1985); H. Barbas, *ibid.* **276**, 313 (1988); _____ and D. N. Pandya, *ibid.* **286**, 353 (1989); M. L. Schwartz and P. S. Goldman-Rakic, *ibid.* **226**, 403 (1984).
24. P. Rakic, *Postgrad. Med. J. Suppl. 1* **54**, 25 (1978); S. A. Bayer and J. Altman, *Exp. Neurol.* **107**, 48 (1990).
25. M. Colombel *et al.*, *Cancer Res.* **52**, 4313 (1992); D. Thomaidou *et al.*, *J. Neurosci.* **17**, 1075 (1997).
26. L. E. Feinendegen, *Tritium-Labeled Molecules in Biology and Medicine* (Academic Press, New York, 1967).
27. A. Barnea and F. Nottebohm, *Proc. Natl. Acad. Sci. U.S.A.* **91**, 11217 (1994); E. Gould, A. Beylin, P. Tanapat, A. Reeves, T. J. Shors, *Nature Neurosci.* **2**, 260 (1999).
28. M. A. Magiakou *et al.*, *Clin. Endocrinol.* **44**, 419 (1996).
29. H. A. Cameron and E. Gould, *Neuroscience* **61**, 203 (1994); E. Gould, H. A. Cameron, D. C. Daniels, C. S. Woolley, B. S. McEwen, *J. Neurosci.* **12**, 3642 (1992).
30. R. F. Martin and D. M. Bowden, *Neuroimage* **4**, 119 (1996).

31. We thank E. Fuchs for help and encouragement, J. Goodhouse for assistance with confocal imaging, and N. Hastings for helpful comments on the manuscript. Supported by NIH grants EY11347-29, MH52423-05, and MH59740-01 and by a grant from the James S. McDonnell Foundation (99-33 CN-QUA.05). Animal care conformed to the regulations of the Princeton University Animal Care and Use Committee.

19 March 1999; accepted 8 September 1999

Yeast Gene for a Tyr-DNA Phosphodiesterase that Repairs Topoisomerase I Complexes

Jeffrey J. Pouliot, Kevin C. Yao, Carol A. Robertson, Howard A. Nash*

Covalent intermediates between topoisomerase I and DNA can become dead-end complexes that lead to cell death. Here, the isolation of the gene for an enzyme that can hydrolyze the bond between this protein and DNA is described. Enzyme-defective mutants of yeast are hypersensitive to treatments that increase the amount of covalent complexes, indicative of enzyme involvement in repair. The gene is conserved in eukaryotes and identifies a family of enzymes that has not been previously recognized. The presence of this gene in humans may have implications for the effectiveness of topoisomerase I poisons, such as the camptothecins, in chemotherapy.

Topoisomerases are cellular enzymes that are crucial for replication and readout of the genome; they work by breaking the DNA backbone, allowing or encouraging topological change, and resealing the break (*1*). The enzymes are efficient because DNA breakage is accompanied by covalent union between protein and DNA to create an intermediate that is resolved during the resealing step. This mechanism, although elegant, also makes topoisomerases potentially dangerous. If the resealing step fails, a normally transient break

Laboratory of Molecular Biology, National Institute of Mental Health, Building 36, Room 1B08, Bethesda, MD 20892–4034, USA.

*To whom correspondence should be addressed. E-mail: nash@codon.nih.gov